

Proximal algorithms for large-scale statistical modeling and optimal sensor/actuator selection

Armin Zare, Neil K. Dhingra, Mihailo R. Jovanović, and Tryphon T. Georgiou

Abstract

Several problems in modeling and control of stochastically-driven dynamical systems can be cast as regularized semi-definite programs. We examine two such representative problems and show that they can be formulated in a similar manner. The first, in statistical modeling, seeks to reconcile observed statistics by suitably and minimally perturbing prior dynamics. The second, seeks to optimally select sensors and actuators for control purposes. To address modeling and control of large-scale systems we develop a unified algorithmic framework using proximal methods. Our customized algorithms exploit problem structure and allow handling statistical modeling, as well as sensor and actuator selection, for substantially larger scales than what is amenable to current general-purpose solvers.

Index Terms

Actuator selection, sensor selection, sparsity-promoting estimation and control, method of multipliers, nonsmooth convex optimization, proximal methods, regularization for design, semi-definite programming, structured covariances.

I. INTRODUCTION

Convex optimization has had tremendous impact on many disciplines, including system identification and control design [1]–[7]. The forefront of research points to broadening the range of applications as well as sharpening the effectiveness of algorithms in terms of speed and scalability. The present paper focuses on two representative control problems, statistical control-oriented modeling and sensor/actuator selection, that are cast as convex programs. A range of modern applications require addressing these over increasingly large parameter spaces, placing them outside the reach of standard solvers. A contribution of the paper is to formulate such problems as regularized semi-definite programs (SDPs) and to develop customized optimization algorithms that scale favorably with size.

Modeling is often seen as an inverse problem where a search in parameter space aims to find a parsimonious representation of data. For example, in the control-oriented modeling of fluid flows, it is of interest to improve upon dynamical equations arising from first-principle physics (e.g., linearized Navier-Stokes equations), in order to accurately replicate observed statistical features that are estimated from data. To this end, a perturbation of the prior model can be seen as a feedback gain that results in dynamical coupling between a suitable subset of parameters [8], [9]. On the flip side, active control of large-scale and distributed systems requires judicious placement of sensors and actuators which again can be viewed as the selection of a suitable feedback or Kalman gain. In either modeling or control, the selection of such gain matrices must be guided by optimality criteria as well as simplicity (low rank or sparse architecture). We cast both types of problems as optimization problems that utilize suitable convex

Financial support from the National Science Foundation under Awards CMMI 1739243, ECCS 1509387 and 1739210, the Air Force Office of Scientific Research under FA9550-16-1-0009 and FA9550-17-1-0435, and ARO under W911NF-17-1-0429 are gratefully acknowledged.

A. Zare and M. R. Jovanović are with the Department of Electrical Engineering, University of Southern California, Los Angeles, CA 90089. N. K. Dhingra is with the Department of Electrical and Computer Engineering, University of Minnesota, Minneapolis, MN 55455. T. T. Georgiou is with the Department of Mechanical and Aerospace Engineering, University of California, Irvine, CA 92697. E-mails: armin.zare@usc.edu, dhin0008@um.edu, mihailo@usc.edu, tryphon@uci.edu.

surrogates to handle complexity. The use of such surrogates is necessitated by the fact that searching over all possible architectures is combinatorially prohibitive.

Applications that motivate our study require scalable algorithms that can handle large-scale problems. While the optimization problems that we formulate are SDP representable, e.g., for actuator selection, worst-case complexity of generic solvers scales as the sixth power of the sum of the state dimension and the number of actuators. Thus, solvers that do not exploit the problem structure cannot cope with the demands of such large-scale applications. This necessitates the development of customized algorithms that are pursued herein.

Our presentation is organized as follows. In Section II, we describe the modeling and control problems that we consider, provide an overview of literature and the state-of-the-art, and highlight the technical contribution of the paper. In Section III, we formulate the *minimum energy covariance completion* (control-oriented modeling) and *sensor/actuator selection* (control) problems as nonsmooth SDPs. In Section IV, we present a customized Method of Multipliers (MM) algorithm for covariance completion. An essential ingredient of MM is the proximal gradient method which we also use for sensor/actuator selection. In Section V, we offer two motivating examples for actuator selection and covariance completion and discuss computational experiments. We conclude with a brief summary of the results and future directions in Section VI.

II. MOTIVATING APPLICATIONS AND CONTRIBUTION

We consider dynamical systems with additive stochastic disturbances. In the first instance, we are concerned with a modeling problem where the statistics are not consistent with a prior model that is available to us. In that case, we seek to modify our model in a parsimonious manner (a sparse and structured perturbation of the state matrix) so as to account for the partially observed statistics. In the second, we are concerned with the control of such stochastic dynamics via a collection of judiciously placed sensors and actuators. Once again, the architecture of the (now) control problem calls for the selection of sparse matrix gains that effect control and estimation. These problems are explained next.

A. Statistical modeling and covariance completion

It is well-established that the linearized Navier-Stokes equations driven by stochastic excitation can account for qualitative [10]–[13] and quantitative [9] features of shear fluid flows. The goal has been to provide insights into the underlying physics as well as to guide control design. A significant advance was achieved recently by recognizing the value of nontrivial stochastic excitation; in [9], it was shown that *colored-in-time* noise can account for features of the flow field that *white* noise (used in earlier literature) cannot [14]. Furthermore, it has been pointed out that the effect of colored-in-time excitation is *equivalent* to a structural perturbation of the system dynamics subject to white-in-time excitation [8], [9]. Such structural perturbations may reveal important dynamical couplings between states and, thereby, enhance understanding of basic physics [9, Section 6.1].

Based on this last point, an optimal state-feedback synthesis problem was formulated in [15] to identify such dynamical couplings that bring consistency with the observed statistics. The principle of parsimony dictates a penalty on the complexity of such model perturbations. To this end, a convex optimization problem can be formulated that is reminiscent to optimal sensor and actuator selection [16], [17]. This type of problem involves a composite cost function of the form

$$f(K, X) + \gamma g(K), \quad (1a)$$

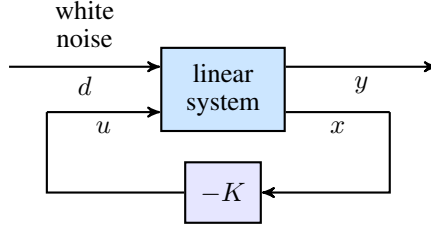


Fig. 1. A feedback connection of an LTI system with a static gain matrix that is designed to account for the sampled steady-state covariance X .

subject to stability of the system in Fig. 1. Here, X denotes a state covariance matrix and K is a state-feedback matrix. The state covariance may be partially known, in which case the constraint

$$X_{ij} = G_{ij} \text{ for } (i, j) \in \mathcal{I}. \quad (1b)$$

is added, where the entries of G represent partially available second-order statistics, i.e., known entries of X for indices in \mathcal{I} . The function $f(K, X)$ penalizes variance and control energy while $g(K)$ is a sparsity-promoting regularizer which penalizes the number of nonzero rows in K ; sparsity in the rows of K amounts to a low rank perturbation of the system dynamics.

The resulting minimum-control-energy covariance completion problem can be cast as an SDP which, for small-size problems, is readily solvable using standard software. We note that similar problems have been considered by complementary viewpoints, aiming at stochastic control [18]–[21] and output covariance estimation [22]–[24].

B. Sensor and actuator selection

The selection of sensors and actuators affects the performance of any closed-loop control system. For large-scale systems with complex dynamical interactions, sensor/actuator selection and placement is a nontrivial task, potentially having combinatorial complexity. To this end, previous work has mostly focused on employing heuristics. The two most popular trends involve greedy algorithms and convex relaxations.

The benefit of a particular selection of sensors/actuators is commonly quantified by properties of the resulting controllability/observability gramians. This correspondence between a choice of sensors/actuators and performance metric has been approached using concepts of submodularity/supermodularity in an attempt to provide guarantees of near-optimality [25], [26]. Unfortunately, metrics on the quality of Kalman filtering estimation – a key component of most designs – appear to lack supermodularity [27]. To make things worse, even selection of open-loop actuators based on average control energy is not supermodular. Such problems may not be effectively addressed by greedy selection methods [28]. In spite of reported initial successes [29], this realization may eventually hamper the use of greedy approaches for sensor/actuator selection.

In addition to greedy algorithms, convex or non-convex methods have also been proposed. In [30], a convex formulation is provided for sensor selection in problems with linear measurements. In [31], sensor selection for correlated measurement noise was approached by maximizing the trace of the Fisher information matrix subject to energy constraints. The placement of power measurement units in power networks was formulated as a variation of the optimal experiment design in [32]. Actuator selection via genetic algorithms was explored in [33]. A non-convex formulation of the joint sensor and actuator placement was provided in [34], [35] and it was recently applied to the linearized Ginzburg-Landau equation [36]. Herein, we consider the problem of the optimal selection of a subset of

available sensors or actuators which, similar to the modeling problem described earlier, involves minimization of nonsmooth composite function of the form (1a).

The sparsity-promoting framework introduced in [37]–[39] can be effectively used to obtain block-sparse structured feedback/observer gains as well as select actuators/sensors. Indeed, algorithms developed in [39] have been used for sensor selection in target tracking [40] and periodic sensor scheduling in networks of dynamical systems [41]. However, these algorithms have been developed for general problems and do not exploit a certain hidden convexity in sensor/actuator selection. Indeed, for the design of row-sparse feedback gains, the authors of [16] introduced a convex SDP reformulation of the problem formulated in [39]. Inspired by [39], the authors of [42] also provided an SDP formulation for the \mathcal{H}_2 and \mathcal{H}_∞ sensor/actuator placement problems for discrete time LTI systems. Their approach utilizes standard solvers for SDPs with re-weighted ℓ_1 norm regularizers. In this paper, we borrow group sparsity regularizers from statistics [43] and develop efficient customized algorithms for the resulting SDPs.

C. Main contribution

We build on the structural similarity between statistical modeling and sensor/actuator selection to develop a unified algorithmic framework for handling large-scale applications. Due to the non-differentiability of the sparsity-promoting term $g(K)$ in the associated cost, standard descent methods are not applicable. We address this issue by utilizing proximal algorithms. For sensor/actuator selection, the alternating direction method of multipliers (ADMM) has been previously used to solve similar problems [17]. In contrast to interior point methods for solving the sensor selection SDP, which scale with the sum of problem dimension and number of available sensors, the ADMM algorithm of [17] only scales with the problem dimension. This is desired when a large pool of sensors/actuators is considered. However, the proposed ADMM algorithm involves subproblems that are difficult to solve and is thus not well-suited for large-scale systems. Herein, we further exploit the problem structure, implicitly handle the stability constraint on state covariances and controller gains by expressing one in terms of the other, and utilize a customized proximal gradient algorithm that scales with the third power of the state-space dimension. Issues like step-size selection, stopping conditions, and initialization are also considered. Finally, numerical experiments are presented to demonstrate the effectiveness of our approach relative to existing methods.

III. PROBLEM FORMULATION

Consider a linear time-invariant (LTI) system with state-space representation

$$\begin{aligned}\dot{x} &= Ax + B_1 d + B_2 u \\ y &= Cx\end{aligned}\tag{2}$$

where $x(t) \in \mathbb{C}^n$ is the state vector, $y(t) \in \mathbb{C}^p$ is the output, $u(t) \in \mathbb{C}^m$ is the control input, $d(t)$ is a stationary zero-mean stochastic process with covariance Ω , B_1 and $B_2 \in \mathbb{C}^{n \times m}$ are input matrices with $m \leq n$, $C \in \mathbb{C}^{p \times n}$ is the output matrix, and the pair (A, B_2) is controllable.

For the applications that we consider, the matrix A in (2) is known and the input matrices B_1 and B_2 are predetermined full column-rank matrices. The goal is to design an optimal feedback control law, $u = -Kx$, such that the closed loop system shown in Fig. 1,

$$\dot{x} = (A - B_2 K)x + B_1 d\tag{3}$$

can account for a set of partially available state-correlations and/or is stable in the \mathcal{H}_2 optimal control sense. More specifically, it is desired to limit the input control energy and steady-state variance of LTI system (2),

$$\lim_{t \rightarrow \infty} \mathbf{E} (x^*(t) Q x(t) + u^*(t) R u(t)), \quad (4)$$

where $\mathbf{E}(\cdot)$ is the expectation operator, $Q = Q^* \succeq 0$ is the state weight, and $R = R^* \succ 0$ specifies the penalty on the control input. On the other hand, parsimony dictates a penalty on the size and directionality of state-feedback couplings. For this, optimal control laws that use a limited number of input channels can be obtained by minimizing composite cost functions of the form

$$f(K, X) + \gamma g(K), \quad (5)$$

where

$$f(K, X) := \text{trace}(Q X + K^* R K X),$$

and $g(K)$ is a regularizing term that promotes row-sparsity of the feedback gain matrix K , subject to the structural constraint

$$(A - B_2 K)X + X(A - B_2 K)^* + B_1 \Omega B_1^* = 0.$$

This constraint represents the steady-state Lyapunov equation for the feedback loop and it relates the matrix K to the steady-state covariance matrix of the state vector

$$X := \lim_{t \rightarrow \infty} \mathbf{E} (x(t) x^*(t)).$$

A. Minimum-input-energy covariance completion

In many applications, due to experimental or numerical limitations, only partial correlations between a limited number of state components are available. Moreover, it is often the case that the origin and directionality of disturbances that generate the statistics is unknown. It is thus desired to design an optimal state feedback control law, $u = -Kx$, such that the closed loop system (3) accounts for the partially available statistics.

For system (2) the steady-state covariance matrix of the state vector X satisfies the following rank condition [44]:

$$\text{rank} \begin{bmatrix} A X + X A^* & B_2 \\ B_2^* & 0 \end{bmatrix} = \text{rank} \begin{bmatrix} 0 & B_2 \\ B_2^* & 0 \end{bmatrix}.$$

This implies that any positive-definite matrix X is admissible as a covariance of LTI system (2) if the input matrix B_2 is full row rank [44], which thereby eliminates the role of the dynamics inherent in A . It is thus important to limit the rank of the input matrix B_2 and to restrict the number of degrees of freedom that are directly influenced by the state-feedback in (3). One way to accomplish this is to minimize the number of input channels or columns of the input matrix B_2 that perturb the dynamical generator A in (3); see [8], [9] for details. This can be equivalently accomplished by minimizing the number of non-zero rows in the matrix K ; if the i th row of K is identically equal to 0, the i th column of B_2 is not used. In addition, the feedback gain K is chosen to minimize both the control energy and fluctuation energy in statistical steady-state, and at the same time, account for partially known second-order statistics. Following [15], we propose the minimum-control-energy covariance completion problem in

its general form as

$$\begin{aligned}
& \underset{K, X}{\text{minimize}} && \text{trace}(QX + K^*RKX) + \gamma \sum_{i=1}^n w_i \|e_i^* K\|_2 \\
& \text{subject to} && (A - B_2K)X + X(A - B_2K)^* + V = 0 \\
& && (CXC^*) \circ E - G = 0 \\
& && X \succ 0,
\end{aligned} \tag{6}$$

where we have employed tools from the paradigm of group-sparsity [43] to augment the performance index $f(K, X)$ with a term that promotes row-sparsity of the feedback gain matrix K . Here, $\gamma > 0$ specifies the importance of sparsity, w_i are nonzero weights, e_i is the i th unit vector in \mathbb{R}^m , $V := B_1\Omega B_1^*$ with Ω as the covariance of the white noise process d , and matrices A , B_1 , B_2 , C , E , G , and Ω are problem data. On the other hand, hermitian matrix $X \in \mathbb{C}^{n \times n}$ and the feedback gain matrix $K \in \mathbb{C}^{m \times n}$ are optimization variables. Entries of matrix G represent partially available second-order statistics of the output y , the symbol \circ denotes elementwise matrix multiplication, and E is the structural identity matrix,

$$E_{ij} = \begin{cases} 1, & \text{if } G_{ij} \text{ is available} \\ 0, & \text{if } G_{ij} \text{ is unavailable.} \end{cases}$$

By identifying a subset of critical input channels in B_2 , problem (6) allows us to uncover the precise dynamical feedback interactions that are required to reconcile the available covariance data with the given linear dynamics.

B. Actuator selection

As is well-known, the unique optimal control law that minimizes the steady-state variance (4) of system (2) is a static state-feedback $u = -Kx$. The optimal gain K and the corresponding state covariance X can be obtained by solving

$$\begin{aligned}
& \underset{K, X}{\text{minimize}} && \text{trace}(QX + K^*RKX) \\
& \text{subject to} && (A - B_2K)X + X(A - B_2K)^* + V = 0 \\
& && X \succ 0.
\end{aligned} \tag{7}$$

Here, $V = B_1\Omega B_1^*$, matrices A , B_1 , B_2 , and Ω are problem data, while $X = X^* \in \mathbb{C}^{n \times n}$ and $K \in \mathbb{C}^{m \times n}$ are optimization variables. The solution can also be obtained by solving an algebraic Riccati equation arising from the KKT conditions of problem (7). We note that, in general, K has no particular structure (i.e., K has no zero entries) and therefore all “input channels” (entries of u) are active and non-zero.

Similar to the covariance completion problem (6), a control law that uses only a subset of available actuators can be sought by promoting row-sparsity of K via a suitable regularizer, as in the following problem

$$\begin{aligned}
& \underset{K, X}{\text{minimize}} && \text{trace}(QX + K^*RKX) + \gamma \sum_{i=1}^n w_i \|e_i^* K\|_2 \\
& \text{subject to} && (A - B_2K)X + X(A - B_2K)^* + V = 0 \\
& && X \succ 0.
\end{aligned} \tag{8}$$

Remark 1: Optimization problem (8) for actuator selection is a special case of optimization problem (6) when the set of known second-order statistics is empty, i.e., the matrices E and G in (6) are zero. In Section IV, we

show that problem (8) arises as a subproblem in the customized method of multipliers algorithm that we propose for solving problem (6).

C. Sensor Selection

The sensor selection problem can be viewed as the dual of the actuator selection problem and can thus be approached in a similar manner. Consider LTI system (2) where the output is corrupted by additive white noise η ,

$$y = Cx + \eta.$$

If (A, C) is an observable pair, the observer

$$\begin{aligned}\dot{\hat{x}} &= A_s \hat{x} + L(y - \hat{y}) \\ &= A_s \hat{x} + LC(x - \hat{x}) + L\eta\end{aligned}$$

provides an estimate \hat{x} of the state x . Here, y represents measurement data, L the observer gain, and $\hat{y} := C\hat{x}$ the predicted output. When $A_s - LC$ is Hurwitz, the zero-mean estimate of x is given by \hat{x} . The Kalman gain minimizes the \mathcal{H}_2 norm of $x - \hat{x}$, i.e., the variance amplification from process and measurement noise to estimation error. Similar to the linear quadratic regulator, the Kalman gain matrix L is obtained by solving a Riccati equation and, in general, has no particular structure and uses all available measurements.

Designing a Kalman filter which uses a subset of the available sensors is equivalent to designing a column-sparse Kalman gain matrix L . Similar to the actuator selection problem, we promote *column-sparsity* via regularization. This amounts to the optimization problem

$$\begin{aligned}\underset{L, X}{\text{minimize}} \quad & \text{trace}(V_s X + L\Omega_\eta L^* X) + \gamma \sum_{i=1}^n w_i \|L e_i\|_2 \\ \text{subject to} \quad & (A_s - LC)^* X + X(A_s - LC) + I = 0 \\ & X \succ 0\end{aligned}\tag{9}$$

where γ , w_i , e_i are as described in problem (8), $V_s := B_1 \Omega B_1^*$, and Ω_η is the covariance of a white stochastic process η . Here, A_s , C , V_s , and Ω are problem data and L and X are the optimization variables.

By setting the problem data in (8) to

$$\begin{aligned}A &= A_s^*, & B_2 &= C^*, & Q &= V_s, \\ V &= I, & R &= \Omega,\end{aligned}$$

the solution to sensor selection problem (9) can be obtained from the solution to actuator selection problem (8) as X and $L = K^*$. Because of this duality, in the remainder of the paper we focus on solving problem (9) as a special case of (8).

D. Change of variables and SDP representation

The hermitian matrix X is positive definite and therefore invertible. Thus, the standard change of variables $Y := KX$ and the equivalence between the row-sparsity of K and the row-sparsity of Y [16] can be utilized to

bring problems (6) and (8) to the following SDP representable form,

$$\begin{aligned}
& \underset{X, Y}{\text{minimize}} \quad \text{trace} \left(QX + Y^* R Y X^{-1} \right) + \gamma \sum_{i=1}^n w_i \|e_i^* Y\|_2 \\
& \text{subject to} \quad AX + XA^* - BY - Y^*B^* + V = 0 \\
& \quad (1 - \delta) [(CXC^*) \circ E - G] = 0 \\
& \quad X \succ 0,
\end{aligned} \tag{10}$$

where

- $\delta = 0$ for covariance completion; and
- $\delta = 1$ for actuator selection.

From the solution of these problems, the optimal feedback gain matrix can be recovered as $K = YX^{-1}$. The convexity of problem (10) follows from the convexity of its objective function and the linearity of its constraint set [4].

Problem (10) can be solved efficiently using general-purpose solvers for small-size problems. To address larger problems, we next exploit the problem structure to develop optimization algorithms based on the proximal gradient algorithm and the method of multipliers.

IV. CUSTOMIZED ALGORITHMS

In this section, we describe the steps through which we solve optimization problem (10), identify the essential input channels in B_2 , and subsequently refine the solutions based on the identified sparsity structure. For notational compactness, we write the linear constraints in (10) as

$$\begin{aligned}
\mathcal{A}_1(X) - \mathcal{B}(Y) + V &= 0 \\
(1 - \delta) [\mathcal{A}_2(X) - G] &= 0
\end{aligned}$$

where the linear operators $\mathcal{A}_1: \mathbb{C}^{n \times n} \rightarrow \mathbb{C}^{n \times n}$, $\mathcal{A}_2: \mathbb{C}^{n \times n} \rightarrow \mathbb{C}^{p \times p}$ and $\mathcal{B}: \mathbb{C}^{m \times n} \rightarrow \mathbb{C}^{n \times n}$ are given by

$$\begin{aligned}
\mathcal{A}_1(X) &:= AX + XA^* \\
\mathcal{A}_2(X) &:= (CXC^*) \circ E \\
\mathcal{B}(Y) &:= B_2Y + Y^*B_2^*.
\end{aligned}$$

A. Elimination of variable X

For any Y , there is a unique X that solves the equation

$$\mathcal{A}_1(X) - \mathcal{B}(Y) + V = 0$$

if and only if the matrices A^* and $-A$ do not have any common eigenvalues [45]. When this condition holds, we can express the variable X as a linear function of Y ,

$$X(Y) = \mathcal{A}_1^{-1}(\mathcal{B}(Y) - V), \tag{11}$$

and restate optimization problem (10) as

$$\begin{aligned} & \underset{Y}{\text{minimize}} && f(Y) + \gamma g(Y) \\ & \text{subject to} && (1 - \delta) [\mathcal{A}_2(X(Y)) - G] = 0 \\ & && X(Y) \succ 0. \end{aligned} \quad (12)$$

The smooth part of the objective function in (12) is given by

$$f(Y) := \text{trace}(Q X(Y) + Y^* R Y X^{-1}(Y))$$

and the regularizing term is

$$g(Y) := \sum_{i=1}^n w_i \|e_i^* Y\|_2.$$

Since problem (12) is equivalent to (10) constrained to the linear subspace defined by (11), it remains convex.

Remark 2: When the matrix A is Hurwitz, expression (11) can be cast in terms of the well-known integral representation,

$$X(Y) = \int_0^\infty e^{At} (V - B Y - Y^* B^*) e^{A^* t} dt.$$

Even for unstable open loop systems, the operator \mathcal{A}_1 is invertible if the matrices A^* and $-A$ do not have any common eigenvalues. In our customized algorithms, we numerically evaluate action of \mathcal{A}_1^{-1} on the current iterate by solving the corresponding Lyapunov equation.

Remark 3: Even in cases where the matrix X cannot be expressed via (11), since (A, B_2) is a controllable pair we can center the design variable around a stabilizing controller K_0 , i.e., by letting $K := K_0 + K_1$, where K_0 is held fixed and K_1 is the design variable. Based on this, the change of variables introduced in Section III-D yields $Y = K_0 X + K_1 X := K_0 X + Y_1$ and $X(Y_1) = \hat{\mathcal{A}}_1^{-1}(\mathcal{B}(Y_1) - V)$ with

$$\hat{\mathcal{A}}_1(X) := (A - B_2 K_0) X + X (A - B_2 K_0)^*. \quad (13)$$

We note that the resulting optimization problem involves a nonsmooth term g which is not separable in the design variable Y_1 ,

$$\begin{aligned} & \underset{Y_1}{\text{minimize}} && \hat{f}(Y_1) + \gamma g(Y_1 + K_0 X(Y_1)) \\ & \text{subject to} && (1 - \delta) [\mathcal{A}_2(X(Y_1)) - G] = 0 \\ & && X(Y_1) \succ 0 \end{aligned}$$

where

$$\begin{aligned} \hat{f}(Y_1) := & \text{trace}(Q X(Y_1)) + \\ & \text{trace}((Y_1 + K_0 X(Y_1))^* R (Y_1 + K_0 X(Y_1)) X^{-1}). \end{aligned}$$

Although convex, $g(Y_1 + K_0 X(Y_1))$ does not have an easily computable proximal operator, making it difficult to apply algorithms that are based on proximal methods.

In such cases one may assume that a given subset of input channels \mathcal{I} will *always* be chosen and that the pair (A, B_2^0) is stabilizable when B_2^0 contains columns that correspond to the input channels represented by \mathcal{I} . It would

thus be desired to select input channels from the complement of \mathcal{I} via the following optimization problem

$$\begin{aligned} & \underset{Y_1}{\text{minimize}} && \hat{f}(Y_1) + \gamma \hat{g}(Y_1) \\ & \text{subject to} && (1 - \delta) [\mathcal{A}_2(X(Y_1)) - G] = 0 \\ & && X(Y_1) \succ 0 \end{aligned}$$

where the operator $\hat{\mathcal{A}}_1$ in (13) is now defined by fixed matrices B_2^0 and K_0 with K_0 being a feedback gain matrix with row-sparsity structure corresponding to \mathcal{I} . The regularization term $\hat{g} := \sum_{i \notin \mathcal{I}} w_i \|e_i^* Y\|_2$ is used to impose row-sparsity on the *remaining* input channels $i \notin \mathcal{I}$ and has an easily computable proximal operator, thus facilitating the use of proximal methods. It is noteworthy that this approach may also be employed to obtain an operator $\hat{\mathcal{A}}_1$ which is better conditioned than \mathcal{A}_1 .

The alternative approach would be to avoid this problem altogether by not expressing X as a function of Y and directly dualizing the Lyapunov constraint on X and Y via augmented Lagrangian based methods, e.g., ADMM [17]. However, as we show in Section V, such approaches do not lead to algorithms that are computationally efficient for all problems.

B. Proximal gradient method for actuator selection

The proximal gradient (PG) method generalizes gradient descent to composite minimization problems in which the objective function is the sum of a differentiable and non-differentiable component [46]. It is most effective when the proximal operator [47] associated with the nondifferentiable component is easy to evaluate; many common regularization functions, such as the ℓ_1 penalty, nuclear norm, and hinge loss, satisfy this condition.

The PG method for solving (12) with $\delta = 1$ is given by

$$Y^{k+1} := \mathbf{prox}_{\beta_k g}(Y^k - \alpha_k \nabla f(Y^k)), \quad (14)$$

where k is the iteration counter, Y^k is the k th iterate, $\alpha_k > 0$ is the step-size, $\beta_k := \alpha_k \gamma$, and $\mathbf{prox}_{\beta g}(\cdot)$ is the proximal operator associated with the function g

$$\mathbf{prox}_{\beta g}(V) := \underset{Y}{\operatorname{argmin}} \quad g(Y) + \frac{1}{2\beta} \|Y - V\|_F^2. \quad (15)$$

Here, $\|\cdot\|_F$ is the Frobenius norm and, for row-sparsity regularizer, the proximal operator is determined by the soft-thresholding operator which acts on the rows of the matrix V ,

$$\mathcal{S}_\beta(e_i^* V) = \begin{cases} (1 - \beta/\|e_i^* V\|_2) e_i^* V, & \|e_i^* V\|_2 > \beta w_i \\ 0, & \|e_i^* V\|_2 \leq \beta w_i. \end{cases}$$

Proximal update (14) results from a local quadratic approximation of f at iteration k , i.e.,

$$\begin{aligned} Y^{k+1} := \underset{Y}{\operatorname{argmin}} \quad & f(Y^k) + \langle \nabla f(Y^k), Y - Y^k \rangle + \\ & \frac{1}{2\alpha_k} \|Y - Y^k\|_F^2 + \gamma g(Y), \end{aligned} \quad (16)$$

followed by a completion of squares that brings the problem into the form of (15). Here, $\langle \cdot, \cdot \rangle$ denotes the standard matricial inner product $\langle M_1, M_2 \rangle := \operatorname{trace}(M_1^* M_2)$ and the expression for the gradient of $f(Y)$ is provided in Appendix A. We note that PG is a special case of proximal Newton-type methods [48], [49], in which the Hessian of the smooth function f is approximated by the scaled identity $(1/\alpha_k)I$.

1) *Choice of step-size in (14)*: At each iteration of the PG method, we determine the step-size α_k via an adaptive Barzilai-Borwein (BB) initial step-size selection [50], i.e.,

$$\alpha_k = \begin{cases} \alpha_m & \text{if } \alpha_m/\alpha_s > 1/2 \\ \alpha_s - \alpha_m/2 & \text{otherwise} \end{cases} \quad (17)$$

followed by backtracking to ensure sufficient descent of the objective function and positive definiteness of $X(Y^{k+1})$; similar strategies were used in [46, Theorem 3.1]. Here, the so-called “steepest descent” step-size α_s and the “minimum residual” step-size α_m are given by [51],

$$\alpha_s = \frac{\langle Y^k - Y^{k-1}, Y^k - Y^{k-1} \rangle}{\langle Y^k - Y^{k-1}, \nabla f(Y^k) - \nabla f(Y^{k-1}) \rangle},$$

$$\alpha_m = \frac{\langle Y^k - Y^{k-1}, \nabla f(Y^k) - \nabla f(Y^{k-1}) \rangle}{\langle \nabla f(Y^k) - \nabla f(Y^{k-1}), \nabla f(Y^k) - \nabla f(Y^{k-1}) \rangle}.$$

If $\alpha_s < 0$ or $\alpha_m < 0$, the step-size from the previous iteration is used; see [50, Section 4.1] for additional details.

2) *Stopping criterion*: We employ a combined stopping condition that terminates the algorithm when either the relative residual

$$r_r^{k+1} = \frac{\|r^{k+1}\|}{\max\{\|\nabla f(Y^{k+1})\|, \|\frac{\hat{Y}^{k+1} - Y^{k+1}}{\alpha_k}\|\} + \epsilon_r},$$

or the normalized residual

$$r_n^{k+1} = \frac{\|r^{k+1}\|}{\|r^1\| + \epsilon_n},$$

are smaller than a desired tolerance. Here, ϵ_r and ϵ_n are small positive constants, the residual is defined as

$$r^{k+1} := \nabla f(Y^{k+1}) + \frac{\hat{Y}^{k+1} - Y^{k+1}}{\alpha_k},$$

and $\hat{Y}^{k+1} := Y^k - \alpha_k \nabla f(Y^k)$. While achieving a small r_r guarantees a certain degree of accuracy, its denominator nearly vanishes when $\nabla f(x^*) = 0$, which happens when $0 \in \partial g(Y^*)$. In such cases, $\|r_n\|$ provides an appropriate stopping criterion; see [50, Section 4.6] for additional details.

3) *Convergence of PG*: The proximal gradient algorithm converges with rate $1/k$ for a fixed step-size $\alpha_k \in (0, 1/L]$ [46], where L is the Lipschitz constant of ∇f . Adaptive step-size selection methods [46], [50] can be used to further enhance performance.

C. Method of multipliers for covariance completion

We handle the additional constraint in the covariance completion problem by employing the Method of Multipliers (MM). MM is the dual ascent algorithm applied to the augmented Lagrangian and it is widely used for solving constrained nonlinear programming problems [52]–[54].

The MM algorithm for constrained optimization problem (12) with $\delta = 0$ is given by,

$$Y^{k+1} := \underset{Y}{\operatorname{argmin}} \mathcal{L}_{\rho_k}(Y; \Lambda^k) \quad (18a)$$

$$\Lambda^{k+1} := \Lambda^k + \rho_k (\mathcal{A}_2(X(Y^{k+1})) - G), \quad (18b)$$

Algorithm 1 Customized PG Algorithm

input: $A, B_1, B_2, \Omega, Q, R, \gamma > 0$, positive constants ϵ_r, ϵ_n , tolerance ϵ , and backtracking constant $b \in (0, 1)$.
initialize: $k = 0, \alpha_{0,0} = 1, r_r^0 = 1, r_n^0 = 1$, choose $Y_0 = K_c X_c$ where K_c and X_c solve the algebraic Riccati equation that specifies the optimal centralized controller.
while: $r_r^k > \epsilon$ or $r_n^k > \epsilon$
 compute α_k : largest feasible step in $\{b^j \alpha_{k,0}\}_{j=0,1,\dots}$
 such that $X(Y^{k+1}) \succ 0$ and Y^{k+1} gives sufficient
 descent in the objective value
 compute r_r^{k+1} and r_n^{k+1}
 $k = k + 1$
 choose $\alpha_{k,0}$ based on (17)
endwhile
output: ϵ -optimal solutions, Y^{k+1} and $X(Y^{k+1})$.

where \mathcal{L}_ρ is the associated augmented Lagrangian,

$$\begin{aligned} \mathcal{L}_\rho(Y; \Lambda) = & f(Y) + \gamma g(Y) + \\ & \langle \Lambda, \mathcal{A}_2(X(Y)) - G \rangle + \frac{\rho}{2} \|\mathcal{A}_2(X(Y)) - G\|_F^2, \end{aligned}$$

$\Lambda \in \mathbb{C}^{p \times p}$ is the Lagrange multiplier and ρ is a positive scalar. The algorithm terminates when the primal and dual residuals are small enough. The primal residual is given as

$$\Delta_p = \|\mathcal{A}_2(X(Y^{k+1})) - G\|_F, \quad (19a)$$

and the dual residual corresponds to the stopping criterion on subproblem (18a)

$$\Delta_d = \min\{r_r, r_n\}, \quad (19b)$$

where the relative and normal residuals, r_r and r_n , are described in Section IV-B.

1) *Solution to the Y -minimization problem (18a):* For fixed $\{\rho_k, \Lambda^k\}$, minimizing the augmented Lagrangian with respect to Y amounts to finding the minimizer of $\mathcal{L}_{\rho_k}(Y; \Lambda^k)$ subject to $X(Y) \succ 0$. Since $g(Y)$ is nonsmooth, we cannot use standard gradient descent methods to find the update Y^{k+1} . However, similar to Section IV-B, a PG method can be used to solve this subproblem iteratively

$$Y^{j+1} = \text{prox}_{\beta_j g}(Y^j - \alpha_j \nabla F(Y^j)), \quad (20)$$

where j is the inner PG iteration counter, $\alpha_j > 0$ is the step-size, $\beta_j := \alpha_j \gamma$, and $F(Y)$ denotes the smooth part of the augmented Lagrangian $\mathcal{L}_{\rho_k}(Y; \Lambda^k)$,

$$\begin{aligned} F(Y) := & f(Y) + \langle \Lambda^k, \mathcal{A}_2(X(Y)) - G \rangle + \\ & \frac{\rho_k}{2} \|\mathcal{A}_2(X(Y)) - G\|_F^2. \end{aligned} \quad (21)$$

The expression for the gradient of $F(Y)$ is provided in Appendix B. Similar to Section IV-B, we combine BB step-size initialization with backtracking to ensure sufficient descent of $\mathcal{L}_{\rho_k}(Y; \Lambda^k)$ and positive definiteness of $X(Y^{j+1})$.

2) *Lagrange multiplier update and choice of step-size in (18b)*: Customized MM for covariance completion is summarized as Algorithm 2. We follow the procedure outlined in [54, Algorithm 17.4] for the adaptive update of ρ_k . This procedure allows for inexact solutions of subproblem (18a) and a more refined update of the Lagrange multiplier Λ through the adjustment of convergence tolerances on Δ_p and Δ_d .

Algorithm 2 Customized MM Algorithm

input: $A, B_1, B_2, C, E, G, \Omega, \gamma > 0$, and tolerances ϵ_p and ϵ_d .

initialize: $k = 0, \rho_0 = 1, \rho_{\max} = 10^9, \epsilon_0 = 1/\rho_0, \eta_0 = \rho_0^{-0.1}$, choose $Y_0 = K_c X_c$ where K_c and X_c solve the algebraic Riccati equation that specifies the optimal centralized controller.

for $k = 0, 1, 2, \dots$

solve (18a) using a similar PG algorithm to Algorithm 1

such that $\Delta_d \leq \epsilon_k$.

if $\Delta_p \leq \eta_k$

if $\Delta_p \leq \epsilon_p$ and $\Delta_d \leq \epsilon_d$

stop with approximate solution Y^{k+1}

else

$$\Lambda^{k+1} = \Lambda^k + \rho_k (\mathcal{A}_2(X(Y^{k+1})) - G)$$

$$\rho_{k+1} = \rho_k, \quad \eta_{k+1} = \max\{\eta_k \rho_{k+1}^{-0.9}, \epsilon_p\}$$

$$\epsilon_{k+1} = \max\{\epsilon_k / \rho_{k+1}, \epsilon_d\}$$

endif

else

$$\Lambda^{k+1} = \Lambda^k$$

$$\rho_{k+1} = \{5\rho_k, \rho_{\max}\}, \quad \eta_{k+1} = \max\{\rho_{k+1}^{-0.1}, \epsilon_p\}$$

$$\epsilon_{k+1} = \max\{1/\rho_{k+1}, \epsilon_d\}$$

endif

endfor

output: optimal solutions, Y^{k+1} and $X(Y^{k+1})$.

D. Computational complexity

Computation of the gradient in both algorithms involves computation of X from Y based on (11), a matrix inversion, and solution to the Lyapunov equation, which each take $O(n^3)$ operations, as well as an $O(mn^2)$ matrix-matrix multiplication. The proximal operator for the function g amounts to computing the 2-norm of all m rows of a matrix with n columns, which takes $O(mn)$ operations. These steps are embedded within an iterative backtracking procedure for selecting the step-size α . If the step-size selection takes q_1 inner iterations and it takes q_2 iterations for the gradient based method to converge, the total computation cost for a single iteration of our customized algorithms is $O(q_1 q_2 n^3)$. In contrast, the worst-case complexity of standard SDP solvers is $O(n^6)$.

E. Comparison with other methods

One way of dealing with the lack of differentiability of the objective function in (12) is to split the smooth and nonsmooth parts over separate variables and to add an additional equality constraint to couple these variables. This

allows for the minimization of the augmented Lagrangian via the the Alternating Direction Method of Multipliers (ADMM) [55].

In contrast to splitting methods, the algorithms considered in this paper use the PG method to solve the nonsmooth problem in terms of the primal variable Y , thereby avoiding the necessity to update additional auxiliary variables and their corresponding Lagrange multipliers. Moreover, it is important to note that the performance of augmented Lagrangian-based methods is strongly influenced by the choice of ρ . In contrast to ADMM, there are principled adaptive rules for updating the step-size ρ_k in MM. Typically, in ADMM, either a constant step-size is used or the step-size is adjusted to keep the norms of primal and dual residuals within a constant factor of one another [55]. Our computational experiments demonstrate that the customized proximal algorithms considered in this paper significantly outperform ADMM.

Remark 4: In [17], a customized ADMM algorithm was proposed for solving the optimal actuator and sensor selection problem. In this, the structural Lyapunov constraint on X and Y is dualized via the augmented Lagrangian. While this approach avoids the issue underscored in Remark 3, as we show in Section V, it performs poorly in practice. This is because of higher computational complexity ($O(n^5)$ per iteration) of the ADMM algorithm developed in [17].

F. Iterative reweighting and polishing

In optimization problem (10) the weighted ℓ_2 norm is used to promote row sparsity of the matrix Y . This choice is inspired by the exact correspondence between the weighted ℓ_1 norm, i.e., $\sum_i w_i |x_i|$ with $w_i = 1/|x_i|$ for $x_i \neq 0$, and the cardinality function $\text{card}(x)$. Since this choice of weights cannot be implemented, the iterative reweighting scheme was proposed instead in [56]. We follow a similar approach and update the weights using

$$w_i^{j+1} = \frac{1}{\|e_i^* Y^j\|_2 + \epsilon}, \quad (22)$$

where Y^j denotes the solution to problem (10) in the j th reweighting step. The small positive parameter ϵ ensures that the weights are well-defined.

After we obtain the solution to problem (10), we conduct a *polishing* step to refine the solution based on the identified sparsity structure. For this, we consider the system

$$\dot{x} = (A - B_{2,\text{sp}} K)x + B_1 d,$$

where the matrix $B_{2,\text{sp}} \in \mathbb{C}^{n \times q}$ is obtained by eliminating the columns of B_2 which correspond to the identified row sparsity structure of Y , and q denotes the number of retained input channels. For this system, we solve optimization problem (10) with $\gamma = 0$. This step allows us to identify the optimal matrix $Y \in \mathbb{C}^{q \times n}$ and subsequently the optimal feedback gain $K \in \mathbb{C}^{q \times n}$ for a system with a lower number of input control channels. As we demonstrate in our computational experiments, polishing not only reduces the energy of the control input but it can also improve the quality of completion of the covariance matrix X .

V. COMPUTATIONAL EXPERIMENTS

We provide two examples to demonstrate the utility of the optimization framework presented for optimal sensor and actuator selection and covariance completion, in addition to the computational efficiency of our proposed algorithms.

TABLE I
COMPARISON OF DIFFERENT ALGORITHMS (IN SECONDS) FOR DIFFERENT NUMBER OF DISCRETIZATION POINTS n AND $\gamma = 10$.

n	CVX	PG	ADMM
32	12.39	6.2	362.4
64	268.11	51.9	4182.6
128	8873.3	875.8	—
256	—	3872.1	—

A. Actuator selection

The Swift-Hohenberg equation is a partial differential equation that has been widely used as a model for studying pattern formations in hydrodynamics and nonlinear optics [57]. Herein, we consider the linearized Swift-Hohenberg equation around its time independent spatially periodic solution [58]

$$\begin{aligned} \partial_t \psi(t, \xi) = & -(\partial_x^2 + 1)^2 \psi(t, \xi) - c \psi(t, \xi) + f \psi(t, \xi) \\ & + u(t, \xi) + d(t, \xi), \end{aligned}$$

with periodic boundary conditions on a spatial domain $\xi \in [0, 2\pi]$. Here, c is a constant and we assume that $f(\xi) := \alpha \cos(\omega \xi)$ with $\alpha \in \mathbb{R}$. Finite dimensional approximation and diagonalization via the discrete Fourier transform yields the following state-space representation

$$\dot{\psi} = A\psi + u + d. \quad (23)$$

For $c = -0.2$, $\alpha = 2$, and $\omega = 1.25$, the linearized dynamical generator has two unstable modes. We set $Q = I$ and $R = 10I$ and solve the actuator selection problem (problem (10) with $\delta = 1$) for 32, 64, 128 and 256 discretization points and for various values of the regularization parameter γ . For $\gamma = 10$, Table I compares the proposed PG algorithm against CVX [59] and the ADMM algorithm of [17]. Both PG and ADMM were initialized with $Y^0 = K_c X_c$, where K_c and X_c solve the algebraic Riccati equation which specifies the optimal centralized controller. This choice guarantees that $X(Y^0) \succ 0$. All algorithms were implemented in Matlab and executed on a 2.9 GHz Intel Core i5 processor with 16 GB RAM. The algorithms terminate when an iterate achieves a certain distance from optimality, i.e., $\|X^k - X^*\|_F / \|X^*\|_F < \epsilon$ and $\|Y^k - Y^*\|_F / \|Y^*\|_F < \epsilon$. The choice of $\epsilon = 10^{-3}$ guarantees that the value of the objective function is within 0.01% of optimality. For $n = 256$, CVX failed to converge. In this case, iterations are run until the relative or normalized residuals defined in Section IV-B2 become smaller than 10^{-2} .

For $n = 128$ and 256, ADMM did not converge to desired accuracy in reasonable time. Typically, the ADMM algorithm of [17] computes low-accuracy solutions quickly but obtaining higher accuracy requires precise solutions to subproblems. The iterative reweighting scheme of Section IV-F can be used to improve the sparsity patterns that are identified by such low-accuracy solutions. Nonetheless, Fig. 2 shows that even for larger tolerances, PG is faster than ADMM.

As γ increases in problem (10), more and more actuators are dropped and the performance degrades monotonically. For $n = 64$, Fig. 3(a) shows the number of retained actuators as a function of γ and Fig. 3(b) shows the percentage

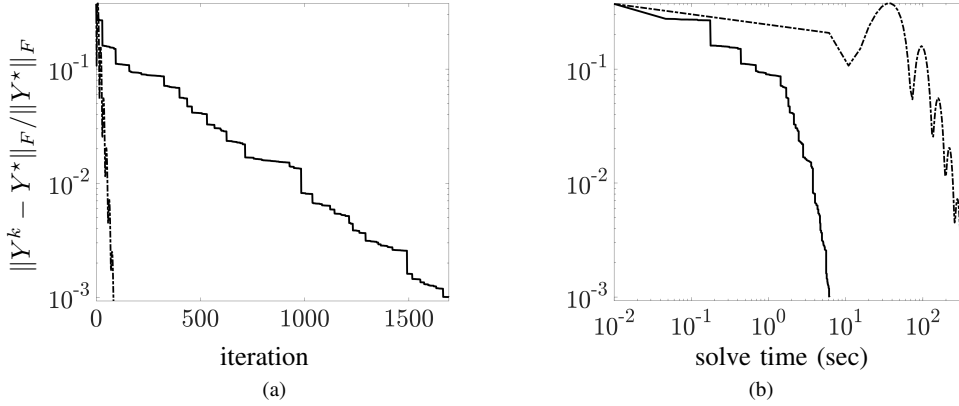


Fig. 2. Convergence curves showing performance of PG (—) and ADMM (---) vs. (a) the number of outer iterations; and (b) solve times for the Swift-Hohenberg problem with $n = 32$ discretization points and $\gamma = 10$. Here, Y^* is the optimal value for Y .

of performance degradation as a function of the number of retained actuators. Figure 3(b) also illustrates that for various numbers of retained actuators, solution to convex optimization problem (10) with $\delta = 1$ consistently yields performance degradation that is no larger than the performance degradation of a greedy algorithm (that drops actuators based on their contribution to the \mathcal{H}_2 performance index). For example, the greedy algorithm leads to 24.6% performance degradation when 30 actuators are retained whereas our approach yields 20% performance degradation for the same number of actuators. This greedy heuristic is summarized in Algorithm 3, where S is the set of actuators and $f(S)$ denotes the performance index resulting from the actuators within the set S . When the individual subproblems for choosing fixed numbers of actuators can be executed rapidly, greedy algorithms provide a viable alternative. There has also been recent effort to prove the optimality of such algorithms for certain classes of problems [29]. However, in our example, the greedy algorithm does not always provide the optimal set of actuators with respect to the \mathcal{H}_2 performance index. Relative to the convex formulation, similar greedy techniques yield suboptimal sensor selection for flexible aircraft wing [7, Section 5.2].

The absence of the sparsity promoting regularizer in (10) leads to the optimal centralized controller which can be obtained from the solution to the algebraic Riccati equation. For $n = 64$, Figs. 4(a) and 4(b) show this centralized feedback gain and the two norms of its rows, respectively. For $\gamma = 0.4$ in (10), 43 of 64 possible actuators are retained and the corresponding optimal feedback gain matrix and row norms are shown in Figs. 4(c) and 4(d). From Figs. 4(b) and 4(c) we see that a truncation of the centralized feedback gain matrix based on its row-norms yields a different subset of actuators than the solution to optimization problem (10).

B. Covariance completion

We provide an example to demonstrate the utility of our modeling and optimization framework for the purpose of completing partially available second-order statistics of a three-dimensional channel flow. In an incompressible channel-flow, the dynamics of infinitesimal fluctuations around the parabolic mean velocity profile, $\bar{\mathbf{u}} = [U(x_2) \ 0 \ 0]^T$ with $U(x_2) = 1 - x_2^2$, are governed by the Navier-Stokes equations linearized around $\bar{\mathbf{u}}$. The streamwise, normal and spanwise coordinates are represented by x_1 , x_2 , and x_3 , respectively; see Fig. 5 for

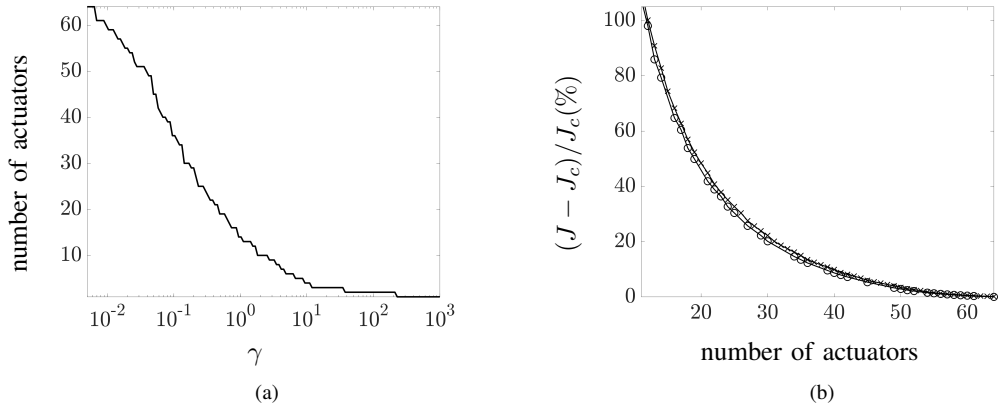


Fig. 3. (a) Number of actuators as a function of the sparsity-promoting parameter γ ; and (b) performance comparison of the optimal feedback controller resulting from the regularized actuator selection problem (\circ) and from the greedy algorithm (\times) for the Swift-Hohenberg problem with $n = 64$.

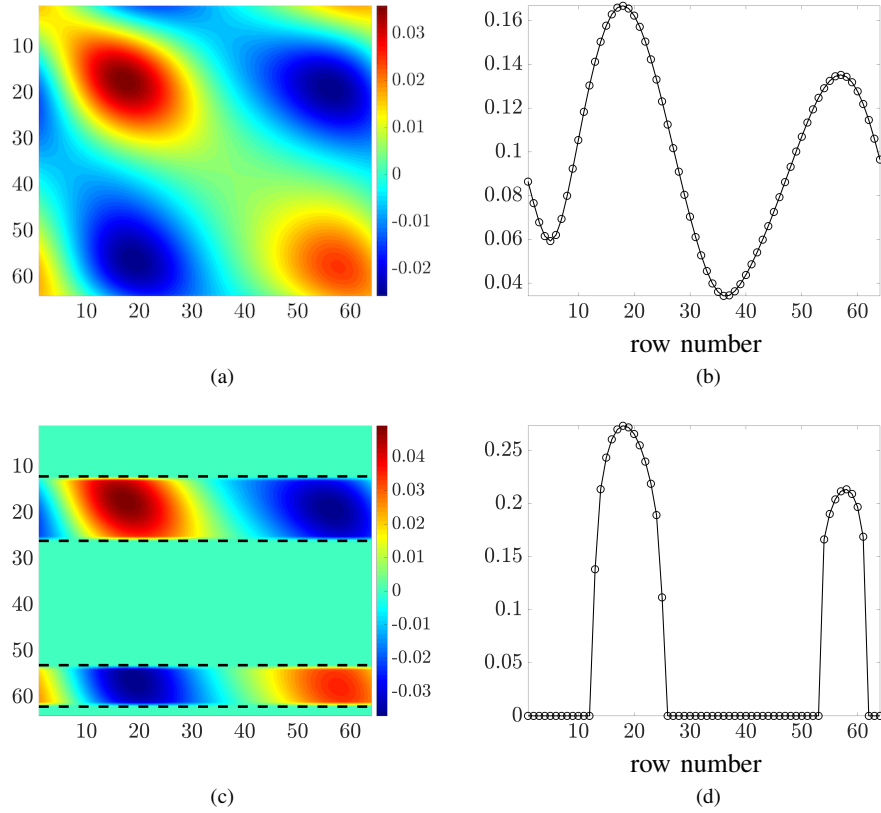


Fig. 4. (a) Optimal centralized feedback gain matrix and (b) its row-norms corresponding to the Swift-Hohenberg dynamics (23) with $n = 64$. (c) The optimal feedback gain matrix and (d) its row-norms resulting from solving problem (10) with $\delta = 1$ and $\gamma = 0.4$ in which the rows between the dashed lines have been retained and polished via optimization.

Algorithm 3 A greedy heuristic for actuator selection

input: $A, B_1, B_2, \Omega, Q, R$.

initialize: $S \leftarrow \{1, \dots, m\}$.

while: $|S| > 0$ and $f(S) < \infty$

$$e^* = \underset{e \in S}{\operatorname{argmin}} f(S) - f(S \setminus \{e\})$$

$$S \leftarrow S \setminus \{e\}$$

endwhile
output: the set of actuators represented by the set S .

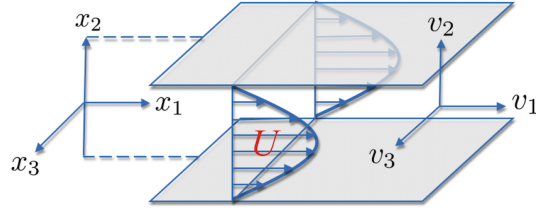


Fig. 5. Geometry of a three-dimensional pressure-driven channel flow.

geometry. Finite dimensional approximation yields the following state-space representation

$$\begin{aligned} \dot{\psi}(\mathbf{k}, t) &= A(\mathbf{k}) \psi(\mathbf{k}, t) + \xi(\mathbf{k}, t), \\ \mathbf{v}(\mathbf{k}, t) &= C(\mathbf{k}) \psi(\mathbf{k}, t). \end{aligned} \quad (24a)$$

Here, $\psi = [v_2^T \ \eta^T]^T \in \mathbb{C}^{2N}$ is the state of the linearized model, v_2 and $\eta = \partial_{x_3} v_1 - \partial_{x_1} v_3$ are the normal velocity and vorticity, the output $\mathbf{v} = [v_1^T \ v_2^T \ v_3^T]^T \in \mathbb{C}^{3N}$ denotes the fluctuating velocity vector, ξ is a stochastic forcing disturbance, $\mathbf{k} = [k_1 \ k_3]^T$ denotes the vector of horizontal wavenumbers, and the input matrix is the identity $I_{2N \times 2N}$. The dynamical matrix $A \in \mathbb{C}^{2N \times 2N}$ and output matrix $C \in \mathbb{C}^{3N \times 2N}$ are described in [12].

We assume that the stochastic disturbance ξ is generated by a low-pass filter with state-space representation

$$\dot{\xi}(\mathbf{k}, t) = -\xi(\mathbf{k}, t) + w(t), \quad (24b)$$

where w denotes a zero mean unit variance white process. The steady-state covariance of system (24) can be obtained as a solution to the Lyapunov equation

$$\tilde{A} \Sigma + \Sigma \tilde{A}^* + \tilde{B} \tilde{B}^* = 0.$$

with

$$\tilde{A} = \begin{bmatrix} A & I \\ O & -I \end{bmatrix}, \quad \tilde{B} = \begin{bmatrix} 0 \\ I \end{bmatrix}, \quad \Sigma = \begin{bmatrix} \Sigma_{11} & \Sigma_{12} \\ \Sigma_{12}^* & \Sigma_{22} \end{bmatrix}.$$

The matrix Σ_{11} denotes the steady-state covariance of system (24a)

$$\Sigma_{11} := \lim_{t \rightarrow \infty} \mathbf{E}(\psi(t) \psi^*(t)),$$

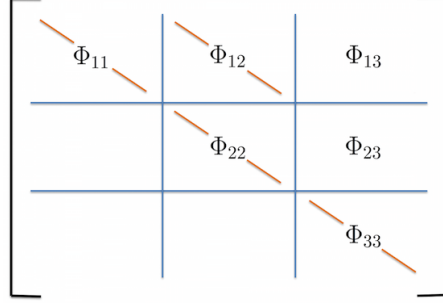


Fig. 6. Structure of the output covariance matrix Φ . Available one-point velocity correlations in the normal direction represent diagonal entries of the blocks in the velocity covariance matrix Φ .

TABLE II
COMPARISON OF DIFFERENT ALGORITHMS (IN SECONDS) FOR DIFFERENT NUMBER OF DISCRETIZATION POINTS N AND $\gamma = 10$.

N	CVX	MM	ADMM
11	9.3	0.19	3.10
21	97.67	5.6	113.4
31	900	7.19	574.44
51	-	34.76	—
101	-	146.51	—

which, at any wavenumber pair \mathbf{k} , is related to the steady-state covariance matrix of the output y via

$$\Phi(\mathbf{k}) = C(\mathbf{k}) \Sigma_{11}(\mathbf{k}) C^*(\mathbf{k}).$$

In this example, we set the covariance of white noise disturbances to the identity ($\Omega = I$) and assume that the one-point velocity correlations, or diagonal entries of the subcovariance matrices in Fig. 6 are available. In order to account for these available statistics, we solve optimization problem (10) with $R = I$ and $Q = 0$ for a state covariance X that agrees with the available statistics.

Computational experiments are conducted for a flow with Reynolds number $Re = 10^3$, the wavenumber pair $(k_1, k_3) = (0, 1)$, for various number of collocation points N in the normal direction (state dimension $n = 2N$), and for various values of the regularization parameter γ . As stated in Algorithm 2, we initialize our algorithms using the optimal centralized controller, $Y^0 := K_c X_c$. This choice guarantees that $X(Y^0) \succ 0$. When CVX can compute the optimal solution of problem (10), for each method iterations are run until the solutions come to within 5% of the CVX solution. For larger problems, iterations are run until the primal and dual residuals satisfy a certain tolerances; $\epsilon_p, \epsilon_d = 10^{-2}$. For $\gamma = 10$, Table II compares various methods based on run times (sec). For $N = 51$ and 101, CVX failed to converge and ADMM did not converge in a reasonable time. Clearly, MM outperforms ADMM. This can also be deduced from Fig. 7, which shows convergence curves for 14 steps of MM and 500 steps of ADMM for $N = 31$ and $\gamma = 10$. For this example, Fig. 8 shows the convergence of MM based on the

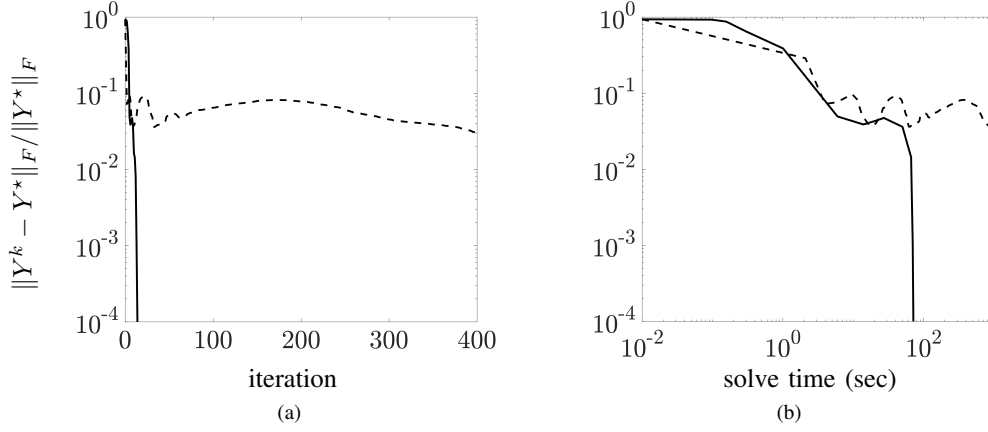


Fig. 7. Convergence curves showing performance of MM (—) and ADMM (---) versus (a) the number of outer iterations; and (b) solve times for $N = 31$ collocation points in the normal direction x_2 and $\gamma = 10$. Here, Y^* is the optimal value for Y .

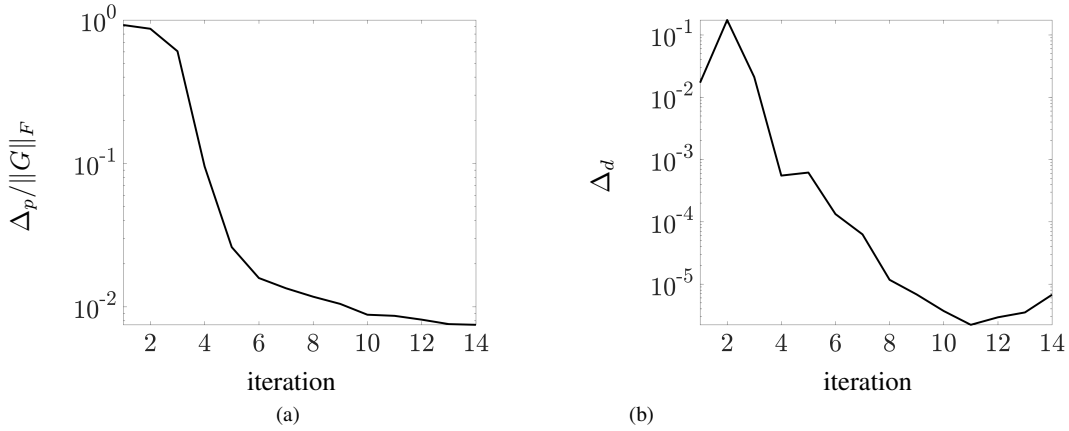


Fig. 8. Performance of MM for the fluids example with $N = 31$ collocation points in the normal direction x_2 and $\gamma = 10$. (a) normalized primal residual; and (b) dual residual based on (19).

normalized primal residual $\Delta_p / \|G\|_F$ and the dual residual Δ_d defined in (19).

We now focus on $N = 51$ collocation points and solve problem (10) for various values of γ . Since the input matrix is assumed to be the identity, the number of inputs in this case is $m = 102$. Figure 9 shows the γ -dependence of the number of retained input channels that result from solving optimization problem (10). As γ increases, more and more input channels are dropped. One of the features of our framework is that covariance completion problem (10) not only determines the number of input channels necessary to satisfy the structural constraints on matrices X and Y , but it also identifies their directionality. Figure 10 shows the input channels that are retained via optimization for different values of γ . This figure illustrates the dominant role of input channels that enter the dynamics of normal velocity and away from the boundaries of the channel. In favor of brevity, we do not expand on the physical interpretations of such findings.

Figures 11(b,d) show the streamwise, and the streamwise/normal two-point correlation matrices resulting from

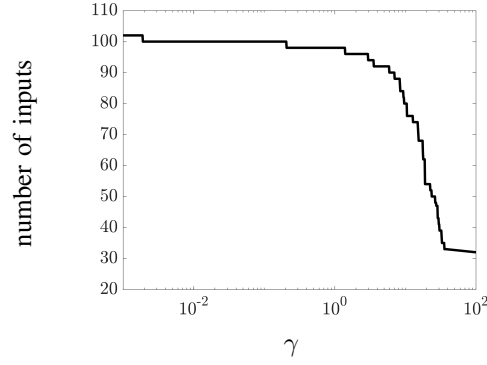


Fig. 9. The γ -dependence of the number of input channels that are retained after solving optimization problem (10) for the channel flow problem with $m = 101$ inputs.

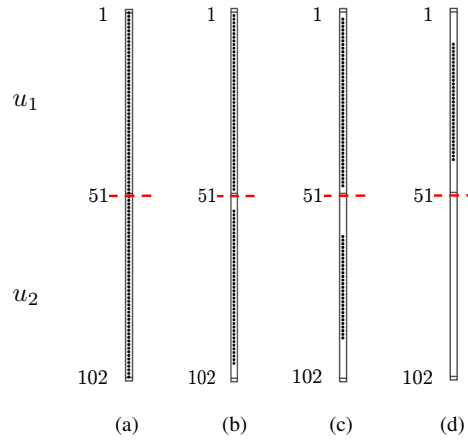


Fig. 10. The input channels in u that remain effective when problem (10) is solved for the channel flow problem with $m = 101$ inputs and (a) $\gamma = 0$, (b) $\gamma = 0.1$, (c) $\gamma = 10$, and (d) $\gamma = 100$.

solving (10) with $\gamma = 100$. Even though only one-point velocity correlations along the main diagonal of these matrices were used as problem data in (10), we observe reasonable recovery of off-diagonal terms of the full two-point velocity correlation matrices and 82% of the original output covariance matrix Φ is recovered. This quality of completion is consistently observed for various values of γ that do not result in the elimination of the critical input channels in the direction of normal velocity, and is an artifact of including the Lyapunov-like constraint in our formulation. This allows us to retain the relevance of the system dynamics and, thereby, the physics of the problem while matching the partially available statistical signatures of the underlying dynamical system; see [8], [9].

VI. CONCLUDING REMARKS

We have examined two problems that arise in modeling and control of stochastically driven dynamical systems. The first addresses the modeling of second-order statistics by a parsimonious perturbation of system dynamics, while the second deals with the optimal selection of sensors/actuators for estimation/control purposes. We have shown that both problems can be viewed as the selection of suitable feedback gains, guided by similar optimality metrics and subject to closed-loop stability constraints. We cast both problems as optimization problems and use

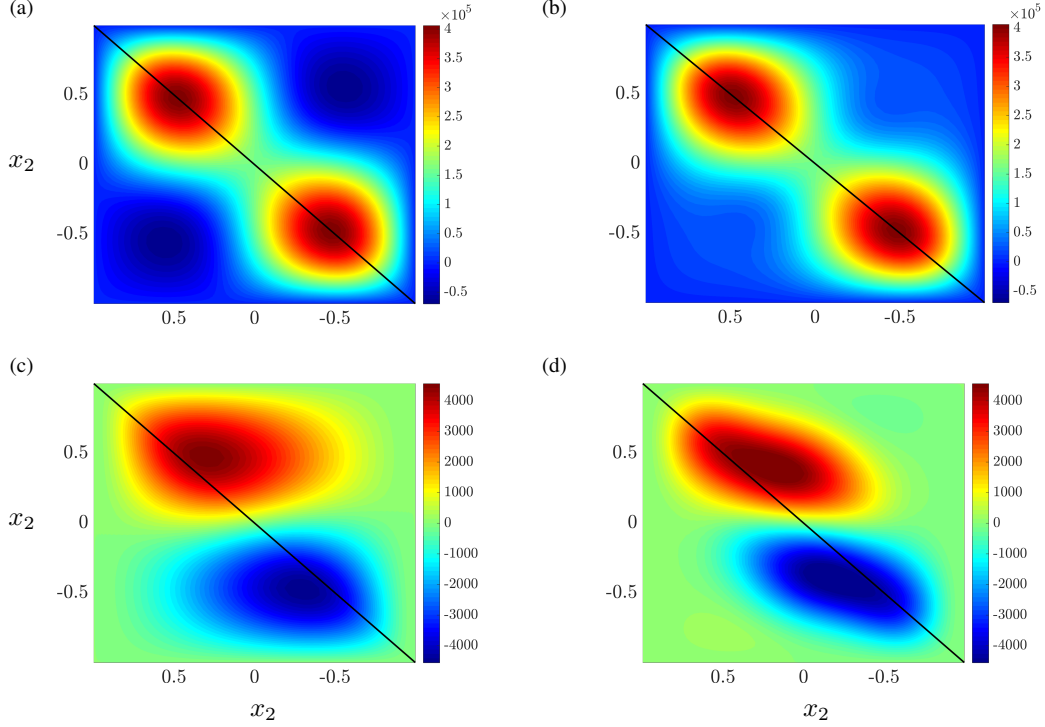


Fig. 11. True covariance matrices of the output velocity field (a, c), and covariance matrices resulting from solving problem (10) (b, d) with $\gamma = 100$ and $N = 51$. (a, b) Streamwise Φ_{11} , and (c, d) streamwise/normal Φ_{12} two-point correlation matrices at $\mathbf{k} = (0, 1)$. One-point correlation profiles that are used as problem data are marked along the main diagonals.

convex surrogates from group-sparsity paradigm to address combinatorial complexity of searching over all possible architectures. While these are SDP representable, the applications that drive our research give rise to the need for scalable algorithms that can handle large problem sizes. We develop a unified algorithmic framework to address both problems using proximal methods. Our algorithms allow handling statistical modeling, as well as sensor and actuator selection, for substantially larger scales than what is amenable to current general-purpose solvers.

In this work, row sparsity is promoted by penalizing a weighted sum of row norms of the feedback gain matrix. While we note that iterative reweighting [56] can improve the row-sparsity patterns determined by this convex approximation of cardinality, the efficacy of more refined approximations, namely low-rank inducing norms [60], [61], for which proximal operators can be efficiently computed, is a subject of future research. Moreover, we will investigate solving these problems via recently developed second order methods for nonsmooth composite optimization problems [49], [62], [63].

APPENDIX

A. Gradient of $f(Y)$ in (14)

To find $\nabla f(Y)$ in (14), we expand $f(Y + \epsilon \tilde{Y})$ around Y for the variation $\epsilon \tilde{Y}$, and collect terms of $O(\epsilon)$. We also account for the variation of X as a result of the variation of Y from

$$(X + \epsilon \tilde{X})^{-1} = X^{-1} - \epsilon X^{-1} \tilde{X} X^{-1} + O(\epsilon^2),$$

and the linear dependence of \tilde{X} on \tilde{Y} , i.e.,

$$\tilde{X} = \mathcal{A}^{-1}(\mathcal{B}(\tilde{Y})).$$

Based on this, at the k th iteration, the gradient of f with respect to Y is given by,

$$\nabla f(Y^k) = 2RY^kX^{-1} - 2B^*(W_2 - W_1),$$

where W_1 and W_2 are solutions to the following Lyapunov equations

$$\begin{aligned} A^*W_1 + W_1A + X^{-1}Y^{k*}RY^kX^{-1} &= 0 \\ A^*W_2 + W_2A + Q &= 0 \end{aligned}$$

Here, X^{-1} denotes the inverse of $X(Y^k)$.

B. Gradient of $F(Y)$ in (20)

Similar to Appendix A, we expand $F(Y + \epsilon\tilde{Y})$ around Y for the variation $\epsilon\tilde{Y}$, and collect terms of $O(\epsilon)$. Based on this, at the k th iteration, the gradient of F with respect to Y is given by,

$$\nabla F(Y^k) = 2Y^kX^{-1} - 2B^*(W_2 + \rho_k W_3 - W_1),$$

where W_1 , W_2 , and W_3 are solutions to the following Lyapunov equations

$$\begin{aligned} A^*W_1 + W_1A + X^{-1}Y^{k*}Y^kX^{-1} &= 0 \\ A^*W_2 + W_2A + \mathcal{A}_2^\dagger(\Lambda^k) &= 0 \\ A^*W_3 + W_3A + \mathcal{A}_2^\dagger(\mathcal{A}_2(X(Y^k)) - G) &= 0 \end{aligned}$$

Here, X^{-1} denotes the inverse of $X(Y^k)$ and the adjoint of the operator \mathcal{A}_2 is given by

$$\mathcal{A}_2^\dagger(\Lambda) := C^*(E \circ \Lambda)C.$$

REFERENCES

- [1] S. Boyd, L. E. Ghaoui, E. Feron, and V. Balakrishnan, *Linear matrix inequalities in system and control theory*. SIAM, 1994.
- [2] G. E. Dullerud and F. Paganini, *A course in robust control theory: a convex approach*. New York: Springer-Verlag, 2000.
- [3] M. Fazel, H. Hindi, and S. Boyd, “A rank minimization heuristic with application to minimum order system approximation,” in *Proceedings of the 2001 American Control Conference*, 2001, pp. 4734–4739.
- [4] S. Boyd and L. Vandenberghe, *Convex optimization*. Cambridge University Press, 2004.
- [5] M. Fazel, H. Hindi, and S. Boyd, “Rank minimization and applications in system theory,” in *Proceedings of the 2004 American Control Conference*, 2004, pp. 3273–3278.
- [6] Z. Liu and L. Vandenberghe, “Interior-point method for nuclear norm approximation with application to system identification,” *SIAM J. Matrix Anal. Appl.*, vol. 31, no. 3, pp. 1235–1256, 2009.
- [7] M. R. Jovanović and N. K. Dhingra, “Controller architectures: tradeoffs between performance and structure,” *Eur. J. Control*, vol. 30, pp. 76–91, July 2016.
- [8] A. Zare, Y. Chen, M. R. Jovanović, and T. T. Georgiou, “Low-complexity modeling of partially available second-order statistics: theory and an efficient matrix completion algorithm,” *IEEE Trans. Automat. Control*, vol. 62, no. 3, pp. 1368–1383, March 2017.
- [9] A. Zare, M. R. Jovanović, and T. T. Georgiou, “Colour of turbulence,” *J. Fluid Mech.*, vol. 812, pp. 636–680, February 2017.
- [10] B. F. Farrell and P. J. Ioannou, “Stochastic forcing of the linearized Navier-Stokes equations,” *Phys. Fluids A*, vol. 5, no. 11, pp. 2600–2609, 1993.
- [11] B. Bamieh and M. Dahleh, “Energy amplification in channel flows with stochastic excitation,” *Phys. Fluids*, vol. 13, no. 11, pp. 3258–3269, 2001.
- [12] M. R. Jovanović and B. Bamieh, “Componentwise energy amplification in channel flows,” *J. Fluid Mech.*, vol. 534, pp. 145–183, July 2005.
- [13] R. Moarref and M. R. Jovanović, “Model-based design of transverse wall oscillations for turbulent drag reduction,” *J. Fluid Mech.*, vol. 707, pp. 205–240, September 2012.
- [14] M. R. Jovanović and B. Bamieh, “Modelling flow statistics using the linearized Navier-Stokes equations,” in *Proceedings of the 40th IEEE Conference on Decision and Control*, 2001, pp. 4944–4949.
- [15] A. Zare, M. R. Jovanović, and T. T. Georgiou, “Perturbation of system dynamics and the covariance completion problem,” in *Proceedings of the 55th IEEE Conference on Decision and Control*, 2016, pp. 7036–7041.
- [16] B. Polyak, M. Khlebnikov, and P. Shcherbakov, “An LMI approach to structured sparse feedback design in linear control systems,” in *Proceedings of the 2013 European Control Conference*, 2013, pp. 833–838.
- [17] N. K. Dhingra, M. R. Jovanović, and Z. Q. Luo, “An ADMM algorithm for optimal sensor and actuator selection,” in *Proceedings of the 53rd IEEE Conference on Decision and Control*, 2014, pp. 4039–4044.
- [18] A. Hotz and R. E. Skelton, “Covariance control theory,” *Int. J. Control*, vol. 46, no. 1, pp. 13–32, 1987.
- [19] K. Yasuda, R. E. Skelton, and K. M. Grigoriadis, “Covariance controllers: A new parametrization of the class of all stabilizing controllers,” *Automatica*, vol. 29, no. 3, pp. 785–788, 1993.
- [20] M. K. K. M. Grigoriadis and R. E. Skelton, “Alternating convex projection methods for covariance control design,” *Int. J. Control*, vol. 60, no. 6, pp. 1083–1106, 1994.
- [21] Y. Chen, T. T. Georgiou, and M. Pavon, “Optimal steering of a linear stochastic system to a final probability distribution, Part II,” *IEEE Trans. Automat. Control*, vol. 61, no. 5, pp. 1170–1180, 2016.
- [22] F. Lin and M. R. Jovanović, “Least-squares approximation of structured covariances,” *IEEE Trans. Automat. Control*, vol. 54, no. 7, pp. 1643–1648, July 2009.
- [23] A. Ferrante, M. Pavon, and M. Zorzi, “A maximum entropy enhancement for a family of high-resolution spectral estimators,” *IEEE Trans. Automat. Control*, vol. 57, no. 2, pp. 318–329, 2012.
- [24] M. Zorzi and A. Ferrante, “On the estimation of structured covariance matrices,” *Automatica*, vol. 48, no. 9, pp. 2145–2151, 2012.
- [25] T. H. Summers, F. L. Cortesi, and J. Lygeros, “On submodularity and controllability in complex dynamical networks,” *IEEE Trans. Control Netw. Syst.*, vol. 3, no. 1, pp. 91–101, 2016.
- [26] V. Tzoumas, M. A. Rahimian, G. J. Pappas, and A. Jadbabaie, “Minimal actuator placement with bounds on control effort,” *IEEE Trans. Control Netw. Syst.*, vol. 3, no. 1, pp. 67–78, 2016.
- [27] H. Zhang, R. Ayoub, and S. Sundaram, “Sensor selection for kalman filtering of linear dynamical systems: Complexity, limitations and greedy algorithms,” *Automatica*, vol. 78, pp. 202–210, 2017.
- [28] A. Olshevsky, “On (non) supermodularity of average control energy,” *IEEE Trans. Control Netw. Syst.*, 2017, doi:10.1109/TCNS.2017.2691463.
- [29] T. Summers, “Actuator placement in networks using optimal control performance metrics,” in *Proceedings of the 55th IEEE Conference on Decision and Control*, 2016, pp. 2703–2708.
- [30] S. Joshi and S. Boyd, “Sensor selection via convex optimization,” *IEEE Trans. Signal Process.*, vol. 57, no. 2, pp. 451–462, 2009.

- [31] S. Liu, S. P. Chepuri, M. Fardad, E. Maşazade, G. Leus, and P. K. Varshney, “Sensor selection for estimation with correlated measurement noise,” *IEEE Trans. Signal Process.*, vol. 64, no. 13, pp. 3509–3522, 2016.
- [32] V. Kekatos, G. B. Giannakis, and B. Wollenberg, “Optimal placement of phasor measurement units via convex relaxation,” *IEEE Trans. Power Syst.*, vol. 27, no. 3, pp. 1521–1530, 2012.
- [33] J. L. Rogers, “A parallel approach to optimum actuator selection with a genetic algorithm,” in *AIAA Guidance, Navigation, and Control Conference*, 2000, pp. 14–17.
- [34] S. Kondoh, C. Yatomi, and K. Inoue, “The positioning of sensors and actuators in the vibration control of flexible systems,” *JSME Int. J., Ser. III*, vol. 33, no. 2, pp. 145–152, 1990.
- [35] K. Hiramoto, H. Doki, and G. Obinata, “Optimal sensor/actuator placement for active vibration control using explicit solution of algebraic Riccati equation,” *J. Sound Vib.*, vol. 229, no. 5, pp. 1057–1075, 2000.
- [36] K. K. Chen and C. W. Rowley, “ \mathcal{H}_2 optimal actuator and sensor placement in the linearised complex Ginzburg-Landau system,” *J. Fluid Mech.*, vol. 681, pp. 241–260, 2011.
- [37] M. Fardad, F. Lin, and M. R. Jovanović, “Sparsity-promoting optimal control for a class of distributed systems,” in *Proceedings of the 2011 American Control Conference*, 2011, pp. 2050–2055.
- [38] F. Lin, M. Fardad, and M. R. Jovanović, “Sparse feedback synthesis via the alternating direction method of multipliers,” in *Proceedings of the 2012 American Control Conference*, 2012, pp. 4765–4770.
- [39] F. Lin, M. Fardad, and M. R. Jovanović, “Design of optimal sparse feedback gains via the alternating direction method of multipliers,” *IEEE Trans. Automat. Control*, vol. 58, no. 9, pp. 2426–2431, September 2013.
- [40] E. Masazade, M. Fardad, and P. K. Varshney, “Sparsity-promoting extended Kalman filtering for target tracking in wireless sensor networks,” *IEEE Signal Process. Lett.*, vol. 19, pp. 845–848, 2012.
- [41] S. Liu, M. Fardad, E. Masazade, and P. K. Varshney, “Optimal periodic sensor scheduling in networks of dynamical systems,” *IEEE Trans. Signal Process.*, vol. 62, no. 12, pp. 3055–3068, 2014.
- [42] U. Münz, M. Pfister, and P. Wolfrum, “Sensor and actuator placement for linear systems based on \mathcal{H}_2 and \mathcal{H}_∞ optimization,” *IEEE Trans. Automat. Control*, vol. 59, no. 11, pp. 2984–2989, 2014.
- [43] M. Yuan and Y. Lin, “Model selection and estimation in regression with grouped variables,” *J. R. Stat. Soc. Series B Stat. Methodol.*, vol. 68, no. 1, pp. 49–67, 2006.
- [44] T. T. Georgiou, “The structure of state covariances and its relation to the power spectrum of the input,” *IEEE Trans. Autom. Control*, vol. 47, no. 7, pp. 1056–1066, 2002.
- [45] R. A. Horn and C. R. Johnson, *Matrix Analysis*. Cambridge University Press, 2012.
- [46] A. Beck and M. Teboulle, “A fast iterative shrinkage-thresholding algorithm for linear inverse problems,” *SIAM J. Imaging Sci.*, vol. 2, no. 1, pp. 183–202, 2009.
- [47] N. Parikh and S. Boyd, “Proximal algorithms,” *Found. Trends Optim.*, vol. 1, no. 3, pp. 123–231, 2013.
- [48] S. Becker and J. Fadili, “A quasi-Newton proximal splitting method,” in *Adv. Neural Inf. Process Syst.*, 2012, pp. 2618–2626.
- [49] J. D. Lee, Y. Sun, and M. A. Saunders, “Proximal Newton-type methods for minimizing composite functions,” *SIAM J. Optim.*, vol. 24, no. 3, pp. 1420–1443, 2014.
- [50] T. Goldstein, C. Studer, and R. Baraniuk, “A field guide to forward-backward splitting with a FASTA implementation,” arXiv:1411.3406, 2014.
- [51] B. Zhou, L. Gao, and Y.-H. Dai, “Gradient methods with adaptive step-sizes,” *Comput. Optim. Appl.*, vol. 35, no. 1, pp. 69–86, 2006.
- [52] D. P. Bertsekas, *Constrained optimization and Lagrange multiplier methods*. New York: Academic Press, 1982.
- [53] D. P. Bertsekas, *Nonlinear programming*. Belmont, MA: Athena Scientific, 1999.
- [54] J. Nocedal and S. J. Wright, *Numerical Optimization*. Springer, 2006.
- [55] S. Boyd, N. Parikh, E. Chu, B. Peleato, and J. Eckstein, “Distributed optimization and statistical learning via the alternating direction method of multipliers,” *Found. Trends Mach. Learn.*, vol. 3, no. 1, pp. 1–122, 2011.
- [56] E. J. Candes, M. B. Wakin, and S. P. Boyd, “Enhancing sparsity by reweighted ℓ_1 minimization,” *J. Fourier Anal. Appl.*, vol. 14, no. 5–6, pp. 877–905, 2008.
- [57] M. C. Cross and P. C. Hohenberg, “Pattern formation outside of equilibrium,” *Rev. Mod. Phys.*, vol. 65, no. 3, p. 851, 1993.
- [58] J. Burke and E. Knobloch, “Localized states in the generalized Swift-Hohenberg equation,” *Phys. Rev. E*, vol. 73, no. 5, p. 056211, 2006.
- [59] M. Grant and S. Boyd, “CVX: Matlab software for disciplined convex programming, version 2.1,” <http://cvxr.com/cvx>, Mar. 2014.
- [60] C. Grussler, A. Zare, M. R. Jovanović, and A. Rantzer, “The use of the r^* heuristic in covariance completion problems,” in *Proceedings of the 55th IEEE Conference on Decision and Control*, 2016, pp. 1978–1983.
- [61] C. Grussler, “Rank reduction with convex constraints,” Ph.D. dissertation, Lund University, 2017.
- [62] N. K. Dhingra, S. Z. Khong, and M. R. Jovanović, “A second order primal-dual method for nonsmooth convex composite optimization,” *IEEE Trans. Automat. Control*, 2017, submitted; also arXiv:1709.01610.
- [63] L. Stella, A. Themelis, and P. Patrinos, “Forward-backward quasi-Newton methods for nonsmooth optimization problems,” *Comput. Optim. Appl.*, vol. 67, no. 3, pp. 443–487, 2017.